Dynamics of photoinduced dichroism and birefringence in optically thick azopolymers

Yu.V. Ponomarev, S.A. Ivanov, Yu.A. Rumyantsev, A.A. Gromchenko

Abstract. **Dynamics of photoinduced dichroism and birefringence have been studied experimentally and theoretically (with the help of the Dumont model) by using some comb-shaped azopolymers. It is shown that the dynamics of trans-isomer concentration and their angular distribution anisotropy can be restored from the experimentally found dichroism dynamics, with the concentration and anisotropy being averaged over the thickness for optically thick samples. At the initial stage of photoinduced anisotropy when the active role of the polymer matrix can be neglected, the experimental time dependence of dichroism is shown to comply well with the Dumont model even if the orientation memory is neglected, provided that only a part of trans-isomers participates in trans-isomerisation.**

Keywords: *azo dye, induced optical anisotropy, dichroism, birefringence.*

1. Introduction

Azopolymers have been investigated intensively for the last 20 years because of a large photoinduced addition to their refractive index, which appears due to photoorientation of azo-dye molecules upon laser irradiation. Under the action of linearly polarised light, azo-dye molecules experience reversible trans-cis transitions. In this case, most trans-isomers oriented in parallel with the direction of light polarisation change to the cis-state, while because of repeated processes of reverse cis-trans-photoisomerisation, rod-like trans-isomers tend to orient perpendicular to the polarisation of the incident light with a hole being burnt in the angular distribution of trans-isomers [1]. As a result, the medium becomes anisotropic (its optical axis is parallel to vector ***E*** of the light wave), which is manifested both in birefringence and dichroism.

Azopolymers are used to fabricate many devices for optical data processing and transmission, e.g. Fresnel lenses [2] and optical switches [3]. They also can be employed to solve the problems of adaptive recovery of the wavefront [4], for recording polarisation holograms with a high diffraction efficiency [5 – 8], and in optical-data storage systems [9 – 12]. When exposed to linearly polarised light, azo-dye molecules incorporated in a liquid crystal can orient liquid-crystal molecules due to intermolecular forces [13, 14]. The operating principle of various optical devices (mirrors [15], lenses [2], optically controlled liquid-crystal displays [16, 17], spatial filters [18]) is based on this effect.

Thus, azo dyes enjoy wide practical application, yet the interaction of light with these materials has not been studied so far. The influence of environmental factors on photo-induced azo-dye reorientation dynamics and mechanism of long-term memory still remain unclear. Many researches widely use the half-phenomenological model proposed by Dumont. Based on balance equations for trans- and cis-isomer concentrations, the model describes reorientation of azo-dye molecules under the action of light [19 – 23]. The model developed in [19, 20] does not take into account the interactions of azo-dye molecules with the polymer matrix and, therefore, does not explain long-lasing anisotropy after the action of the light is terminated. Later, the model was improved: a term has been introduced into the balance equations, which is responsible for the interaction between the azo dye and polymer matrix and is caused by the presence of the mean field [24]. Other ways to account for the influence of the matrix were proposed in papers [22, 23, 25]. Thus, paper [25] puts forward the mechanism of optically induced anisotropy, which does not require the presence of cis-isomers and also involves optical memory. Note that today the Dumont model is best developed. It can claim an adequate description of the dynamics of induced anisotropy at the initial stage of optical excitation. However, using the model requires a large number of adjusting parameters (see, for example, [19 – 23]), which leaves the question about its adequacy open. The other above-mentioned approaches call for more justification and thorough experimental testing.

The aim of this paper is to investigate the dynamics of optical anisotropy (dichroism and birefringence) of a number of azopolymers and to compare experimental results with theoretical results, which are based on the Dumont model.

2. Restoring cis-isomer concentration dynamics and trans-isomer distribution anisotropy from measurements of azopolymer dichroism and birefringence

Consider the influence of radiation linearly polarised along the *z* axis with the frequency ω and intensity *I* propagating along *y* axis on the optical properties of an azopolymer

**Yu.V. Ponomarev, S.A. Ivanov, Yu.A. Rumyantsev,
A.A. Gromchenko** Department of Physics, M.V. Lomonosov Moscow State University, Vorob'evy gory, 119992 Moscow, Russia;
e-mail: ponomarev.yu@mail.ru

(Fig. 1). We assume that cis-isomer molecules are optically isotropic [26], their properties being determined by the absorption cross section σ_c and polarisability α_c. We also assume that trans-isomer molecules are of the rod-like form [27] and in the coordinate system bound to the sample their spatial orientation is described by the unit vector $\boldsymbol{m}(\Omega) = \{\cos\varphi\sin\theta, \sin\varphi\sin\theta, \cos\theta\}$. In these approximations, the optical properties of trans-isomers in the coordinate system bound to a molecule are determined by the absorption ($\hat{\sigma}_t$) and susceptibility ($\hat{\alpha}_t$) tensors with only non-zero zz-components being equal to σ_t and α_t, respectively. We will describe the spatial orientation of trans-isomers with the aid of the angular distribution of their concentration $n_t(\Omega, t)$. Because the optical properties of cis-isomers are isotropic, their concentration $N_c(t)$ is independent of the spatial angle Ω and can be written in the form

$$N_c(t) = N_0 - \int n_t(\Omega, t)d\Omega, \tag{1}$$

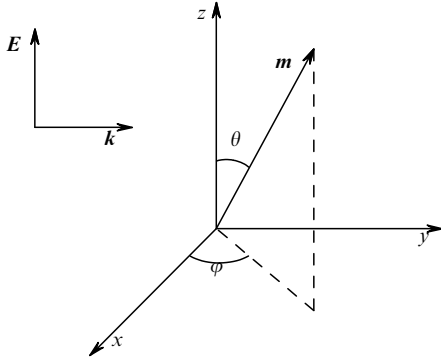where N_0 is the total concentration of azo-dye molecules.

Figure 1. Geometry of interaction of an azo-dye trans-isomer with light in an azopolymer.

During the absorption of light caused by trans-cis-transitions, the angle orientation of trans-isomers and, consequently, the optical properties of the azopolymer change. On the assumption that the absorption of the polymer matrix is negligibly small, the expression for diagonal components β_z, β_x of absorption tensor $\hat{\beta}$ of the azopolymer can be written in the form

$$\beta_i(t) = \sigma_c N_c(t) + \int n_t(\Omega, t)(S^{-1}\hat{\sigma}_t S)_{ii}d\Omega, \quad i = x, z, \tag{2}$$

where S is the matrix of transition from the coordinate system bound to the trans-isomer molecule to the coordinate system bound to the sample; σ_c is the cis-isomer absorption cross section.

Let us expand the angular distribution of the trans-isomer concentration into a series of Legandre polynomials $P_j(\cos\theta)$:

$$n_t(\Omega, t) = \frac{1}{4\pi} N_0 \sum_{j=0}^{M} T_j P_j(\cos\theta). \tag{3}$$

Because of the symmetry of the trans-isomer distribution function $n_t(\theta, t) = n_t(\pi - \theta, t)$, expression (3) will hold only

even-order terms $(j = 0, 2, \ldots, M)$. Coefficients T_j of expansion (3) have simple physical interpretation: $[1 - T_0(t)]$ is the relative concentration of cis-isomers [see expression (1)], and the coefficients at highest terms of the expansion describe the trans-isomer angular distribution anisotropy. If we substitute (3) into (2), we obtain

$$\Delta\beta_z(t) = \left[\left(\sigma_c - \frac{\sigma_t}{3}\right)[1 - T_0(t)] + \frac{2}{15}\sigma_t T_2(t)\right]N_0,$$

$$\Delta\beta_x(t) = \left[\left(\sigma_c - \frac{\sigma_t}{3}\right)[1 - T_0(t)] - \frac{1}{15}\sigma_t T_2(t)\right]N_0, \tag{4}$$

where $\Delta\beta_i(t) = \beta_i(t) - \beta_{0i}$; β_{0i} are the components of the absorption tensor of the non-illuminated azopolymer; $i = x$, z. Assuming that all azo-dye molecules of the non-illuminated azopolymer are in the trans-state and evenly distributed over angles, we have $\beta_0 = \beta_x(0) = \beta_z(0) = \sigma_t N_0/3$. Note that expression (4) holds only two first coefficients of expansion (3), which correspond to the so-called parabolic approximation. We can derive from (4) that

$$1 - T_0(t) = \frac{\Delta\beta_z(t) + 2\Delta\beta_x(t)}{9(\alpha - 1/3)\beta_0},$$

$$T_2(t) = \frac{\Delta\beta_z(t) - \Delta\beta_x(t)}{0.6\beta_0}, \tag{5}$$

where $\alpha = \sigma_c/\sigma_t$.

The ratio α of the absorption cross sections for cis- and trans-isomers can be evaluated by the initial stage of dependences $\Delta\beta_x(t)$ and $\Delta\beta_z(t)$ immediately after the light is on. When the sample is not illuminated, $n_t(\Omega, 0) = N_0/(4\pi)$ and the rate of change in the trans-isomer distribution after the start of the light action can be written for the given geometry in the form

$$\left.\frac{dn_t}{dt}\right|_{t=0} = -\frac{N_0}{4\pi}a_t I\cos^2\theta, \tag{6}$$

where $a_t = \gamma_t\sigma_t/(\hbar\omega)$ and γ_t is the quantum yield of trans-cis-isomerisation. Differentiating (2) with respect to time and using (6), we obtain

$$\left.\frac{d\beta_z}{dt}\right|_{t=0} = (\alpha - 0.6)\frac{\beta_0 a_t I}{4\pi},$$

$$\left.\frac{d\beta_x}{dt}\right|_{t=0} = (\alpha - 0.2)\frac{\beta_0 a_t I}{4\pi}. \tag{7}$$

It follows from (7) that immediately after the light is switched on the behaviour of the functions $\beta_x(t)$ and $\beta_z(t)$ depends on α. Moreover, there are three regions at the initial stage of these dependences where the components of the absorption tensor behave differently:

$$\alpha < 0.2 \left(\left.\frac{d\beta_z}{dt}\right|_{t=0}, \left.\frac{d\beta_x}{dt}\right|_{t=0} < 0\right),$$

$$0.2 < \alpha < 0.6 \left(\left.\frac{d\beta_z}{dt}\right|_{t=0} < 0, \left.\frac{d\beta_x}{dt}\right|_{t=0} > 0\right),$$

$$\alpha > 0.6 \left(\left. \frac{\mathrm{d}\beta_z}{\mathrm{d}t} \right|_{t=0}, \; \left. \frac{\mathrm{d}\beta_x}{\mathrm{d}t} \right|_{t=0} > 0 \right).$$

Thus, the time dependence of the absorption of weak probe radiation whose polarisation is parallel and perpendicular to that of the acting light can be used to determine α and to restore the dynamics of concentration $T_0(t)$ and anisotropy of angular distribution $[T_2(t)]$ of trans-isomers.

Above we considered the case when the sample is optically thin and the change in the intensity of the acting radiation during its propagation through the sample can be neglected. Because the wavelength of the radiation acting on the azopolymer is usually taken within the absorption band of the trans-isomer ($n - \pi^*$ transition), the optical thickness of the sample $K = \beta_0 d$ is usually greater than unit for the acting light. When a sample is optically thick and a photoinduced change of absorption is assumed negligible, the coefficients $T_0(t)$ and $T_2(t)$ in expression (4) should be averaged over the sample thickness d.

Given the above assumptions about isotropy of cis-isomers and the rod-like structure of trans-isomers, the equation for the angular distribution of the trans-isomer concentration in the Dumont model [19, 28] can written in the form [21]:

$$\frac{\partial n_\mathrm{t}(\Omega, t)}{\partial t} = -a_\mathrm{t} n_\mathrm{t}(\Omega, t) I \cos^2 \theta + \frac{1}{4\pi} \left(\frac{1}{\tau_\mathrm{c}} + a_\mathrm{c} I \right)$$
$$\times \left[N_0 - \int n_\mathrm{t}(\Omega', t) \mathrm{d}\Omega' \right] + D \Delta_\Omega n_\mathrm{t}(\Omega, t), \quad (8)$$

where τ_c is the cis-isomer lifetime defined by spontaneous cis-trans transitions; $a_\mathrm{c} = \gamma_\mathrm{c} \sigma_\mathrm{c} / (\hbar\omega)$; γ_c is the quantum yield of cis-trans-isomerisation; D is the rotational diffusion coefficient; Δ_Ω is the Laplacian.

The first term in the right-hand side of (8) describes a decrease in trans-isomers due to their interaction with linearly polarised light, the second – the increase in the trans-isomer concentration caused by both spontaneous and induced cis-trans transitions. The coefficient $1/(4\pi)$ means that the orientation memory is absent during the trans-cis-trans-isomerisation [27]. The last term takes into account the rotational diffusion of trans-isomers.

We will seek the solution of equation (8) in the form of expansion over Legendre polynomials (3). By substituting (3) into (8), we derive equations

$$\frac{\mathrm{d}T_0}{\mathrm{d}t} = - \left(\frac{1}{3} a_\mathrm{t} I + a_\mathrm{c} I + \frac{1}{\tau_\mathrm{c}} \right) T_0 - \frac{2}{15} a_\mathrm{t} I T_2 + \left(a_\mathrm{c} I + \frac{1}{\tau_\mathrm{c}} \right),$$
$$(9)$$

$$\frac{\mathrm{d}T_n}{\mathrm{d}t} = -a_\mathrm{t} I \left[A_{n-2}^{(n)} T_{n-2} + A_n^{(n)} T_n + A_{n+2}^{(n)} T_{n+2} \right] - Dn(n+1) T_n$$

for the expansion coefficients, where n is the positive even integer;

$$A_{n-2}^{(n)} = \frac{n(n-1)}{(2n-3)(2n-1)};$$

$$A_n^{(n)} = \frac{(n+1)^2}{(2n+3)(2n+1)} + \frac{n^2}{(2n+1)(2n-1)};$$

$$A_{n+2}^{(n)} = \frac{(n+1)(n+2)}{(2n+5)(2n+3)}.$$

The initial conditions for the coefficients are $T_0(0) = 1$, $T_n(0) = 0$.

In experiments on photoinduced birefringence dynamics, we measured the phase shift $\Phi(t)$ which is related to optical anisotropy $\Delta n_\mathrm{ind}(t)$ as

$$\Phi(t) = \frac{2\pi}{\lambda} \Delta n_\mathrm{ind}(t) d,$$

where λ is the wavelength of the probe light. When interpreting the experimental results, we should take into account the optical thickness of the sample [29, 30]. For this reason, it was necessary to develop a method for investigating the birefringence dynamics in thick samples ($K \gg 1$). As shown in [31], the exponential relation $\Delta n_\mathrm{ind}(t) = \Delta n_\mathrm{max}[1 - \exp(-t/\tau)]$ (where τ is the birefringence rise time) can be used to describe the birefringence dynamics in thin samples in the first approximation. Using the results of papers [29, 31 – 33], we assume that Δn_max is independent of the intensity of the acting radiation, and τ and I are related as $I\tau = \mathrm{const}$. Taking into account the absorption of the acting light in the polymer sample, we find that

$$\Phi(t) = \frac{2\pi}{\lambda} \frac{\Delta n_\mathrm{max}}{\beta} \int_1^W \left[1 - \exp\left(-\frac{t'}{z} \right) \right] \frac{\mathrm{d}z}{z}, \quad (10)$$

where $t' = t/\tau_0$; τ_0 is the birefringence rise time in the surface layer of the sample; $W = \exp K$. Calculations showed that for $W \to \infty$ relation (10) can be rewritten in the form

$$\Phi(t) = \frac{2\pi}{\lambda} \frac{\Delta n_\mathrm{max}}{\beta} \ln \frac{\gamma t}{\tau_0}, \quad (11)$$

where $\gamma = 1.781$ is the Euler – Mascheroni constant.

Expressions for the tensor components of the refractive index of the azopolymer can be written in the form similar to that of (2). The dependence $T_2(t)$ can be also found from the difference of changes in refractive indices Δn_z, Δn_x for probe light for its two orthogonal polarisations under assumption that Δn_z, $\Delta n_x \ll n_0$:

$$T_2(t) = \frac{\Delta n_z(t) - \Delta n_x(t)}{0.6 n_0}, \quad \Delta n_i(t) = n_i(t) - n_0, \; i = x, z,$$

where n_0 is the refractive index of the unperturbed medium.

3. Experiment

The experimental setup shown in Fig. 2 was used to study the dynamics of photoinduced dichroism in different azopolymers. The output of a 532-nm diode-pumped solid-state LCS-DTL-318 laser was used as the acting light. The induced dichroism was measured with the probe radiation from a solid-state LCM-S-111 laser at the same wavelength. Both probe and acting light were linearly polarised. The dynamics of the absorption coefficient for probe radiation polarised parallel and perpendicular to the polarisation of acting radiation was detected. A half-wave plate was employed to rotate the polarisation plane of the probe light. A cell with a heater and temperature detector, into which samples were placed, allowed us to control the heating of the material in the range from 25 to 80 °C. The
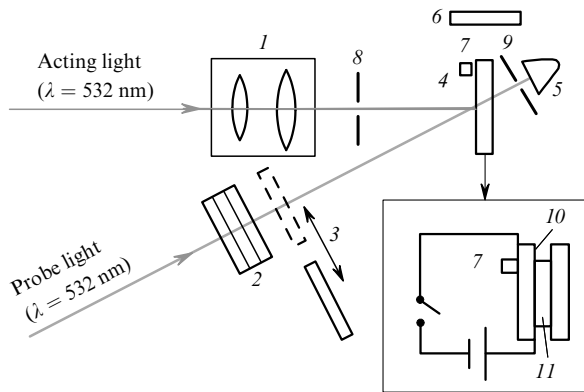
Figure 2. Experimental setup: (*1*) telescope; (*2*) set of filters; (*3*) half-wave plate; (*4*) polymer cell; (*5*) photodetector; (*6*) fan; (*7*) thermal sensor; (*8*, *9*) apertures; (*10*) metal coating; (*11*) sample.

intensity of probe radiation modulated at the frequency 1 kHz and propagated through the sample was detected with a photodetector using the synchronous detection method.

The experimental setup described in [31, 32] was used for investigating the dynamics of photoinduced birefringence. The linearly polarised light of an argon laser ($\lambda = 488$ nm) was used to induce birefringence. The linearly polarised light of a He – Ne laser ($\lambda = 633$ nm) was used to detect photo-induced changes in a polymer film. The angle between the polarisation planes of probe and acting light beams was $45°$. A photodiode and a special detection system were employed to measure the intensity of the probe beam after its passing through the polymer sample and analyser. The results of the measurements were used to determine the phase difference between the orthogonally polarised components of the probe light.

Three polymer samples A, B1, B2 were used to investigate dichroism and birefringence. Polymer A (amorphous azo-compound [34]) was a 0.5% solution of azo-dye (4-4-oxicyanoazobenzene) in PMMA (polymethylmethacrylate). Azo-compounds B1 and B2 (azo-polymers with 100 % azo-dye content) were homopolymers {4-[(methacryloyoxyalkylene)methylamino]-4-X-azobenzene}. In polymer B1 molecule NO_2 replaces X, in polymer B2 it is atom Cl. Samples A, B1 and B2 were 0.8 mm, 1.7 μm and 10 μm thick, respectively. Theoretical and experimental values of parameters for polymer A and B1 are given in Table 1. In calculations of the azo-dye concentration N_0, the density of the samples was taken to be 1.3 g cm^{-3}.

Table 1. Parameters of A and B1 polymers.

Polymer type	N_0/cm^{-3}	β_0/cm^{-1} ($\lambda = 532$ nm)	σ_t/cm^2 ($\lambda = 532$ nm)
A	4×10^{19}	21	1.6×10^{-18}
B1	2.3×10^{21}	14380	1.9×10^{-17}

4. Discussion of the results

Figures 3a and 3b give the experimental time dependences of the absorption coefficient for samples A and B1 when the polarisation of the probe light is perpendicular [$\Delta\beta_x(t)$] and parallel [$\Delta\beta_z(t)$] to the polarisation of the acting light. The measurements were performed at room temperature. The

dynamics of the photoinduced increment to the absorption coefficient exhibits two distinct features. First, at the initial stage the absorption of samples A and B1 changes differently, which can be explained by different ratios of the absorption cross sections of trans- and cis-isomers $\alpha = \sigma_c/\sigma_t$.

The change in the absorption in the initial part of dependences $\Delta\beta_x(t)$ and $\Delta\beta_z(t)$ is related to the appearance of cis-isomers resulting from trans-cis-isomerisation. Because cis-isomers have an isotropic absorption cross section, an increase in their quantity makes the absorption coefficient grow identically both in the case of the perpendicular or parallel polarised radiation. At the same time the falling concentration of trans-isomers decreases the absorption coefficient. Because trans-isomers have an anisotropic absorption cross section, the absorption decreases differently for the light with different polarisations [see (7)]. Linear approximation of the initial part of the dependences allowed us to evaluate α and the quantum yield of trans-cis-isomerisation γ_t for samples A and B1: these values are given in the caption of Fig. 3.

The azo dyes entering into the polymer samples have two characteristic absorption bands. One is related to the $\pi - \pi^*$ electron transition, the other to the $n - \pi^*$ electron transition [35, 36]. In polymer A the $\pi - \pi^*$ transition corresponds to wavelengths $\lambda = 320 - 360$ nm (trans-isomer) and $\lambda \sim 200$ nm (cis-isomer) [36], the $n - \pi^*$ transition is responsible for the band $\lambda = 440 - 460$ nm (this band is the same for trans- and cis-isomers and absorption cross sections σ_t and σ_c are the values of the same order of magnitude). The quantum yield of trans-cis-isomerisation $\gamma_t = 0.21 - 0.24$ for the $n - \pi^*$ transition and 0.1 for the $\pi - \pi^*$ transition. The absorption in the $\pi - \pi^*$ transition band is an order of magnitude higher than the absorption in the $n - \pi^*$ transition band [36].

The results obtained for polymer A ($\alpha = 0.4$, $\gamma_t = 0.15$) agree qualitatively with the data given in [36]. There is no quantitative agreement here because those data refer to azo-dye monomers that are placed in a neutral solvent (n-hexane).

The situation is different for polymers B1 and B2. Here all depends on the degree of polarity of X substitute [35]. If the substitute is non-polar (a hydrogen atom, for example), the absorption spectrum of the azo dye is close to the absorption spectrum of polymer A. With the growing polarity of the substitute, the $\pi - \pi^*$ transition band for trans-isomers moves to a longer-wavelength region and with $X = NO_2$ (maximal polarity) it overlaps the $n - \pi^*$ transition band. The absorption band can take the area from 460 nm to 500 nm in this case [37]. The degree of polarity of the substitute does not have much effect on the spectral characteristics of cis-isomers (no effect in the $n - \pi^*$ transition band [37]). It may be expected therefore that α for polymer B1 will be considerably smaller than for polymer A. Experimental results for polymer B1 ($\alpha = 0.01$, $\gamma_t = 0.11$) qualitatively agree with the data from papers [35, 36].

The estimates of parameters N_0, σ_t and α allowed us to use dependences $\Delta\beta_z(t)$ and $\Delta\beta_x(t)$ to restore the dynamics of the expansion coefficients $T_0(t)$ and $T_2(t)$ (Figs 3c and 3d). Recall that $[1 - T_0(t)]$ is the relative concentration of cis-isomers. Approximation of the initial part of $T_0(t)$ with an exponential function gave the following estimates of the lifetime of cis-isomers: $\tau_c^A = 5.4$ s, $\tau_c^{B1} = 1.7$ s.
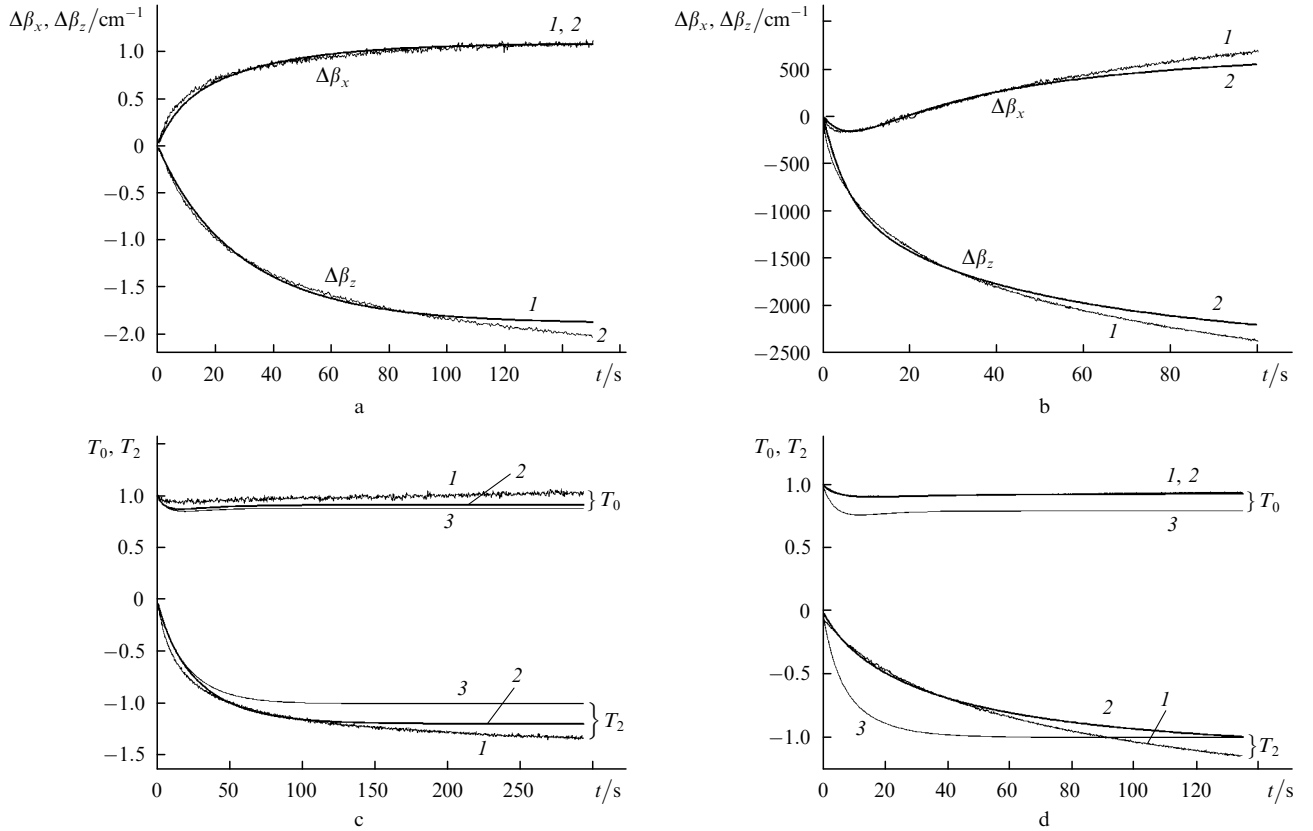
Figure 3. Experimental (*1*) and theoretical (*2, 3*) time dependences of photoinduced increments to the absorption coefficient for the probe light polarisations parallel ($\Delta\beta_z$) and orthogonal ($\Delta\beta_x$) to the polarisation of the acting light (a, b) and coefficients T_0 and T_2 (c, d) for the A polymer at $\gamma_t = \gamma_c = 0.15$, $\alpha = 0.4$, $K = 1.7$, $\tau_c = 12$ s, $D = 10^{-3}$ rad^2 s^{-1}, $\xi = 0.21$, $I = 144$ W cm^{-2} (a, c) and for the B polymer at $\gamma_t = \gamma_c = 0.11$, $\alpha = 0.01$, $K = 3.3$ (*2*) and 0 (*3*), $\tau_c = 7$ s, $D = 10^{-4}$ rad^2 s^{-1}, $\xi = 0.34$, $I = 48$ W cm^{-2} (b, d). In Fig. 3c curve (*2*) is the result of calculations with T_0, T_2, T_4, curve (*3*) – the result of calculations with T_0, T_2.

The thermal relaxation time τ_c of the cis-trans-isomer-isation in polymer B2 was evaluated by analysing the birefringence dynamics. The constant $\Delta n_{max}/\beta$ in expression (11) was used to calculate the birefringence kinetic parameters. This constant takes two different values depending on the exposure (Table 2 and Fig. 4). For the exposure time $t <$ 15 – 20 s, the constant $\Delta n_{max}/\beta$ is greater than it is when the exposure time is $20 < t < 3000$ s. In this case the same time 'boundary' ($t = 15 - 20$ s) is observed for different intensities I of the acting light (photoinduced birefringence was measured for $I = 0.04$ and 0.09 W cm^{-2}). In our opinion it is $t = 15 - 20$ s that is the estimate of time τ_c for a B2 polymer film. The following fact says for this suggestion. Optically thick films ($K > 5$) were used in the experiments on birefringence. In the area of the film where the intensity of the acting light is high enough for the duration of the

reversible trans-cis-trans-isomerisation cycle to be less than the lifetime τ_c, the effect of cis-isomers on the birefringence process cannot be neglected. With a low-intensity field, the cycle has the form of trans-cis-isomerisation – thermal relaxation – trans-isomer, i.e. the effect of cis-isomer on the development of birefringence can be neglected when the intensity of light is small. The intensity $I < 2$ mW cm^{-2} is considered small for B2 polymers.

Table 2. Kinetic parameters of birefringence rise in B1 and B2 polymers.

Polymer type	Process	$\beta_0/\mu m^{-1}$ ($\lambda = 488$ nm)	$\dfrac{\Delta n_{max}}{\beta_0}/\mu m$	Δn_{max} ($\lambda = 632.8$ nm)
	1		0.0095	0.029
B2	2	3	0.0035	0.01
	total		0.013	0.039
B1		10.5	0.01	0.104

N o t e . Birefringence rise in B2 polymer consists of two processes. Process 1 exists for any exposures up to $t = 3000$ s, process 2 exists only for the exposure time $t < 15 - 20$ s. The whole process exists at $t < 20$ s.

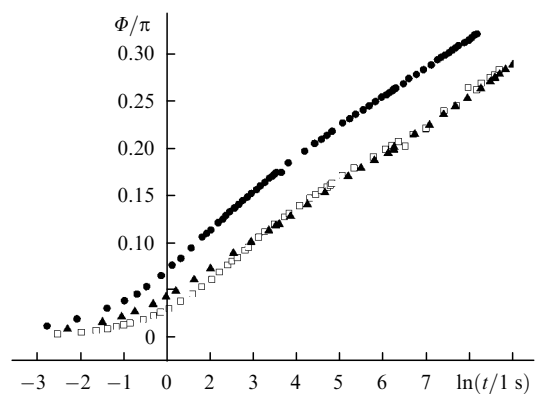**Figure 4.** Photoinduced birefringence dynamics [$\Phi(t)$] for the B1 polymer at the intensity of the light exposure $I = 0.09$ W cm^{-2} (▲) and for the B2 polymer at $I = 0.04$ (□) and 0.09 W cm^{-2} (●).

The estimated cis-isomer lifetime ($\tau_c^A = 5.4$ s, $\tau_c^{B1} = 1.7$ s, $\tau_c^{B2} = 15 - 20$ s) agree qualitatively with the data presented in paper [38] and review [35]. According to [35], the lifetime τ_c is strongly dependent on the degree of polarity of the X substitute in the azo dye. If the substitute has no polarity (X = H, CH_3), a cis-isomer can have a very long lifetime (up to ten days [38]). In the case of a polar substitute (X = NO_2, B1 polymer), the lifetime τ_c is significantly shorter (from a few milliseconds in a solution to a few seconds in a polymer film). The B2 polymer lifetime τ_c seems to take an intermediate value.

In a parabolic approximation, the trans-isomer angular distribution anisotropy is governed by coefficient T_2 and grows monotonically with the exposure time. The approximation of $T_2(t)$ by the dependence $T_2(t) = A_0 \sum_{k=1}^{3} A_k \times \exp(-t/\tau_k)$ gives the following values of parameters A_k and τ_k: $A_0 = -1.41 \pm 0.01$, $A_1 = 0.43 \pm 0.02$, $A_2 = 0.55 \pm 0.01$, $A_3 = 0.42 \pm 0.01$, $\tau_1 = 6.7 \pm 0.3$ s, $\tau_2 = 29 \pm 2.0$ s, $\tau_3 = 165 \pm 14$ s for the A sample and $A_0 = -1.47 \pm 0.04$, $A_1 = 0.04 \pm 0.01$, $A_2 = 0.37 \pm 0.04$, $A_3 = 1.0 \pm 0.01$, $\tau_1 = 5.1 \pm 1.6$ s, $\tau_2 = 23 \pm 3$ s, $\tau_3 = 118 \pm 13$ s for the B1 sample.

The experimental dependences $T_0(t)$ and $T_2(t)$ and the estimates of parameters N_0, σ_t, α, γ_t allowed us to test the Dumont model described by equation (8). In this case, we used three terms of the expansion of the trans-isomer concentration angular distribution in a series of Legendre polynomials. Note that the Dumont model describes the dynamics of trans- and cis-isomers during the action of light on a sample and does not at all describe the memory effect inherent in azopolymers because the model does not allow for the influence of a polymer matrix [22–24].

Equation (8) governs the behaviour of an optically thin azopolymer ($K \ll 1$). When a sample is optically thick ($K > 1$) the light absorption can be easily taken into account if we assume that $\beta_0 = const$, i.e. if we neglect a photoinduced change in the absorption coefficient and divide the medium in N thin layers of thickness δ. Inside each layer l the intensity I_l is considered independent of coordinates and equal to $I_0 \exp(-lK/N)$, where I_0 is the intensity of the light incident on the sample. Solving equations (9) for each layer, we can find the expansion coefficients $T_{0l}(t)$ and $T_{nl}(t)$. The expression for the change in the absorption coefficient of the sample for the probe light is similar to (4), where functions

$$T_0(t) = \frac{1}{N}\sum_{l=1}^{N} T_{0l}(t), \quad T_2(t) = \frac{1}{N}\sum_{l=1}^{N} T_{2l}(t)$$

are averaged over. In the Dumont model the account for the absorption of the acting light by the sample has two consequences: the coefficient $T_2(t)$ reaches a stationary value for a longer time and the stationary value itself becomes smaller.

In the parabolic approximation, the Dumont model has two characteristic times, τ_1 and τ_2 ($\tau_1 \ll \tau_2$). The first (τ_1) is mainly manifested in the dependence $T_0(t)$ and characterises the rise time of the cis-isomer concentration, which is strongly dependent on the intensity of the incident light and the cis-isomer lifetime. The second (τ_2) has effect on $T_2(t)$ and is largely determined by the rotational diffusion. Calculations showed that taking into account higher terms of the expansion results in an increase/decrease in τ_1 and 'splitting' of time τ_2 into a few time periods τ_{2m} whose quantity is determined by the number of the terms of the

expansion M in (3). At the same time, the relation $\tau_{2m} \ll \tau_1$ holds true. Thus, we can assume that irrespective of the number of the terms of expansion (9), the Dumont model is characterised by two effective times, τ_{1eff} and τ_{2eff} ($\tau_{1eff} \ll \tau_{2eff}$). The analysis of the experimental dependences $T_0(t)$ and $T_2(t)$ (Figs 3c and 3d) shows that they can be described by three exponents with characteristic times τ_1, τ_2 and τ_3 ($\tau_1 \ll \tau_2 \ll \tau_3$). In this case, τ_3 is the time that is required for $T_2(t)$ to reach a stationary value. Time τ_3 can reflect the active effect of the polymer matrix on the isomerisation dynamics. If we assume that the matrix has dynamic memory [22–24], time τ_3 can characterise the relaxation time of that memory.

On the assumption that in the Dumont model time τ_2, which is obtained from the approximation of experimental dependence $T_2(t)$, is related to the rotational diffusion, the time necessary for carrying out the testing should not exceed a few τ_2. It was found in this case that the experimental quasi-stationary values of the modulus T_2 are a few times smaller than those given by the model. To eliminate this discrepancy, we introduced the parameter ξ and used the quantity $\beta_0^* = \xi\beta_0$ in relations (5) instead of the absorption coefficient β_0 of the unexposed sample. Thus, the experimental dependences $T_0(t)$ and $T_2(t)$ were fitted to those of the model with the help of two parameters of the model (τ_c and D) and one additional parameter ξ. The other parameters used in the model were estimated (as was described above) by using experimental curves $\Delta\beta_z(t)$ and $\Delta\beta_x(t)$ and additional assumption that $\gamma_c = \gamma_t$.

The results are shown in Fig. 3. Note that the account for more terms in expansion (3) influences the dependences $T_0(t)$ and $T_2(t)$, thus increasing the time interval within which the theoretical curves correspond to the experimental ones. Particularly, given T_4, the time during which we observed only a minor departure of the experimental curve from the theoretical one was about 100 s for the A sample compared to the interval 25 s in the case of the parabolic approximation (Fig. 3c). Absorption in an optically thick sample ($K > 1$) also improves the result of curve fitting (Fig. 3d). Thus, we can state that with the above assumptions about the absorption cross sections of cis- and trans-isomers, the Dumont model describes fairly well the experimental curves at the initial stage of illumination and, therefore, reflects correctly the processes of trans-cis-isomerisation. The parameter ξ has a physical meaning if we assume that not all trans-isomers can participate in trans-cis-isomerisation. Indeed, in the case of an unexposed isotropic sample all azopolymer isomers are in the trans-isomers and they all absorb light. At the same time, only trans-isomers participating in trans-cis-isomerisation are responsible for photoinduced changes in the absorption coefficients $\Delta\beta_z(t)$ и $\Delta\beta_x(t)$, which implies that it is their concentration that should enter into expression (5). For the trans-cis-trans-photoisomerisation cycle to be possible, there should be, in addition to absorption of a quantum of light, a sufficiently large volume of free space around an azo-dye molecule [39, 40]. For example, paper [37] reports that the quantum yield of the trans-cis-isomerisation of an azo-dye in Langmuir–Blodgett films is four orders of magnitude smaller than the quantum yield of the same dye in an organic solvent. For this reason, the introduction of the parameter ξ looks quite reasonable.

5. Conclusions

We have proposed a computation method which makes it possible to determine optical characteristics of azopolymers (absorption cross sections of trans- and cis-isomers σ_t and σ_c, the quantum yield of the trans-cis-isomerisation γ_t) and reconstruct the trans-isomer concentration (T_0) dynamics and anisotropy dynamics of their angular distribution (T_2) by using an experimentally measured dynamics of photo-induced dichroism and birefringence. The method can be applied to optically thin and thick samples.

The dynamics of photoinduced anisotropy has been experimentally studied for two types of amorphous azopolymers. The kinetic parameters of dichroism and birefringence have been defined and the estimates of σ_t, σ_c, γ_t have been obtained. By using these azopolymers we have tested the Dumont model. It has been shown that at the initial stage of photoinduced anisotropy when the active role of the polymer matrix can be neglected, experimental dependences of the dichroism dynamics can be correctly described by the Dumont model even with orientation memory being neglected given the assumption that only a part of trans-isomers participates in trans-isomerisation.

References

1. Todorov T., Nikolova L., Tomova N. *Appl. Opt.*, **23**, 4309 (1991).
2. Lin L.-C., Jau H.-C., Lin T.-H., Fuh A.Y.G. *Opt. Express*, **15** (6), 2900 (2007).
3. Ivanov M., Ilieva D., Minchev G., Petrova T., Dragostinova V., Todorov T., Nikolova L. *Appl. Phys Lett.*, **86**, 181902 (2005).
4. Simonov A.N., Larichev A.V., Shibaev V.P., Stakhanov A.I. *Opt. Commun.*, **197**, 175 (2001).
5. Baklanov E.A., Uraev D.V., Shmalgauzen V.I. *Vest. Mosk. Univer. Ser. Fiz. Astronom.*, (1), 20 (2005).
6. Andruzzi L., Altomare A., Ciardelli F., Solaro R. *Macromolecules*, **32**, 448 (1999).
7. Blanche P.-A., Lemaire Ph.C., Maertens C., Dubois P., Jerome R. *Opt. Commun.*, **185**, 1 (2000).
8. Wang C., Fei H., Yang A., Wei Z., Qui Y., Chen Y. *Opt. Commun.*, **159**, 58 (1999).
9. Dhar L., Curtis K., Tackitt M., Schilling M., Campbell S., Wilson W., Hill A., Boyd C., Levinos N., Harris A. *Opt. Lett.*, **23** (2), 1710 (1998).
10. Kawata S., Kawata Y. *Chem. Rev.*, **100**, 1777 (2000).
11. Ramanujam P.S., Holme C., Hvilsted S., Pedersen M., Andruzzi F., Paci M., Tassi E.L., Magagnini P., Hoffman U., Zebger I., Siesler H.W. *Polym. Advan. Technol.*, **7**, 768 (1996).
12. Loerincz E., Szarvas G., Koppa P., Ujhelyi F., Erdei G., Sueto A., Varhegyi P., Sajti Sz., Kerekes A., Ujvari T., Ramanujam P.S. *Proc. SPIE Int. Soc. Opt. Eng.*, **4991**, 34 (2003).
13. Kiselev A.D., Chigrinov V.G., Huang D.D. *Phys. Rev. E*, **72**, 061703 (2005).
14. Kwok H.-S., Chigrinov V.G., Takada H., Takatsu H. *J. Display Technol.*, **1** (1), 41 (2005).
15. Lin T.-H., Huang Y., Zhou Y., Fuh A.Y.G., Wu S.-T. *Opt. Express*, **14** (10), 4479 (2006).
16. Lin T.-H., Jau H.-C., Hung S.-Y., Fuh H.-R., Fuh A.Y.G. *Appl. Phys. Lett.*, **89**, 021116 (2006).
17. Chigrinov V.G., Kwok H.S., Takada H., Takatsu H. *Proc. SPIE Int. Soc. Opt. Eng.*, **6487**, 64870F (2007).
18. Fuh A.Y.G., Lin T.-S. *Proc. SPIE Int. Soc. Opt. Eng.*, **6487**, 64870E (2007).
19. Dumont M. *Mol. Cryst. Liquid Cryst.*, **282**, 437 (1996).
20. Simonov A.N., Uraev D.V., Shibaev V.P., Kostromin S.G. *Kvantovaya Elektron.*, **32** (2), 143 (2002) [*Quantum Electron.*, **32** (2), 143 (2002)].
21. Simonov A.N., Larichev A.V. *Kvantovaya Elektron.*, **28** (1), 87 (1999) [*Quantum Electron.*, **29** (7), 644 (1999)].
22. Kiselev A.D. *J. Phys: Condens. Matter.*, **14**, 13417 (2002).
23. Yaroshchuk O.V., Kiselev A.D., Zakrevskyy Yu., Bidna T., Kelly J., Chien L.-C., Lindau J. *Phys. Rev. E*, **68**, 011803 (2003).
24. Pedersen T.G., Johansen P.M. *Phys. Rev. Lett.*, **79** (13), 2470 (1997).
25. Chigrinov V., Pikin S., et al. *Phys. Rev. E*, **69**, 061713 (2004).
26. Nikolova L., Markovsky P., Tomova N., Dragostinova V., Mateva N. *J. Mod. Optics*, **35**, 1789 (1988).
27. Huang T., Wagner K.H. *J. Opt. Soc. Am. B*, **13**, 282 (1996).
28. Sekkat Z., Dumont M. *Synth. Met.*, **54**, 373 (1993).
29. Song O.-K., Wang C.H., Pakley M.A. *Macromolecules*, **30**, 6913 (1997).
30. Natansohn A., Rochon P. *Macromolecules*, **31**, 7960 (1998).
31. Shibaev V.P., Kostromin S.G., Ivanov S.A. *High-Molecular Compounds A*, **39**, 43 (1997).
32. Shibaev V.P., Kostromin S.G., Ivanov S.A., in *Polymers as Electrooptical Active Media* (Berlin – Heidelberg – New York: Springer-Verlag, 1997) p. 37.
33. Rasmussen P.H., Ramanujam P.S., Hvilsted S., Berg R.H. *J. Am. Chem. Soc.*, **121**, 4738 (1999).
34. Stakhanov A.I. *Doct. Diss.* (Moscow, Moscow State University, 1999).
35. Delaire J.A., Nakatani K. *Chem. Rev.*, **100**, 1817 (2000).
36. Tamai N., Miyasaka H. *Chem. Rev.*, **100**, 1875 (2000).
37. Schonhoff M., Mertesdorf M., Losche M. *J. Phys. Chem.*, **100**, 7558 (1996).
38. Ramanujam P.S., Hvilsted S., Zebger I., Siesler H.W. *Macromol. Rapid Commun.*, **16** (7), 445 (1995).
39. Mita I., Horie K., Hirao K. *Macromolecules*, **22**, 558 (1989).
40. Ho M.S., Natansohn A., Rochon P. *Macromolecules*, **28**, 6124 (1995).